Annals of Pure and Applied Mathematics
Vol. 3, No. 2, 2013, 142-154
ISSN: 2279-087X (P), 2279-0888(online)
Published on 21 August 2013
www.researchmathsci.org

Annals of
Pure and Applied Mathematics

Unsteady Solutions of Thermal Boundary Layer Equations by using Finite Difference Method

Md. Saidul Islam [1], ***Md. Samsuzzoha*** [2], ***Shamim Ara*** [3] **and** ***Nazmul Islam*** [4]
[1]Department of Mathematics, Faculty of Science, Engineering & Technology
Hamdard University Bangladesh, Bangladesh
[2]Department of Mathematics, Faculty of Engineering & Industrial Science, Swinburne University of Technology, Hawthonn, Victoria-3122, Australia
[3]Department of Mathematics, University of Rajshahi, Rajshahi-6205, Bangladesh
[4]Mathematics Discipline, Khulna University, Khulna-9208, Bangladesh.
Email: saeedmathku@yahoo.com

Received 4 August 2013; accepted 20 August 2013

Abstract. We studied the equation of continuity and derived the Navier-Stockes (N-S) equations of motion for viscous compressible and incompressible fluid flow, Boundary layer and thermal boundary layer equations are then derived. Then we studied unsteady solutions of thermal boundary layer equations. Thermal Boundary layer equations have been non-dimensionalised by using non-dimensional variable and the equations have been derived from Navier-Stokes equation and concentration equation by boundary layer technique. The non-dimensional boundary layer equations are non-linear partial differential equations. These equations are solved by using finite difference method. The solution of heat and mass transfer flow is studied to examine the velocity, temperature and concentration distribution. The effect on the velocity, temperature and concentration profiles for various parameters entering into the problems are separately discussed and shown graphically.

Keywords: Thermal Boundary Layer, Grashof number, Modified Grashof number, Prandlt number, Schmidt number.

AMS Mathematics Subject Classification (2010): 80A20

1. Introduction

An important application of finite differences is in numerical analysis, especially in numerical differential equations, which aim at the numerical solution of ordinary, partial differential and thermal Boundary Layer equations respectively. The idea is to replace the derivatives appearing in the differential equation by finite differences that approximate them. The resulting methods are called finite difference methods. Common applications of the finite difference method are in computational science and engineering disciplines, such as thermal engineering, fluid mechanics, etc.

The unsteady solution of thermal boundary layer equation is one of the most interesting choices to the researcher by using finite difference method. S. V. Patankar and D. B. Spalding, [1] performed. A finite-difference procedure for solving the equations of the two-dimensional boundary layer flow in 1967. M. S. Alam et all.,[2] Studied the mass transfer flow past a vertical porous plate. M. M. Alam et all. [3] performed mass transfer flow in *vertical porous plate.* M. M. Alam et all. [5] investigated combained heat and mass transfer flow. A general, implicit, numerical, marching procedure is presented for the solution of parabolic partial differential equations, with special reference to those of the boundary layer. The main novelty lies in the choice of a grid which adjusts its width so as to conform to the thickness of the layer in which significant property gradients are present. The non-dimensional stream function is employed as the independent variable across the layer.

2. Mathematical model of the flow

By introducing Cartesian coordinate system, the $X-$axis is chosen along the plate in the direction of the flow and the $Y-$axis is normal to it. Initially we consider that the plate as well as the fluid is at the same temperature $T\left(T_\infty\right)$ and the concentration level $C\left(C_\infty\right)$ everywhere in the fluid is same. Also it is considered that the fluid and the plate is at rest after that the plate is to be moving with a constant velocity. U_0 in its own plane and instantaneously at time t > 0, the species concentration and the temperature of the plate are raised to $C_w\left(>C_\infty\right)$ and $T_w\left(>T_\infty\right)$ respectively, which are there after maintained constant, where C_w, T_w are species concentration and temperature at the wall of the plate and C_∞, T_∞ are the concentration and temperature of the species far away from the plate respectively. The physical model of the study is shown in Fig. 1.

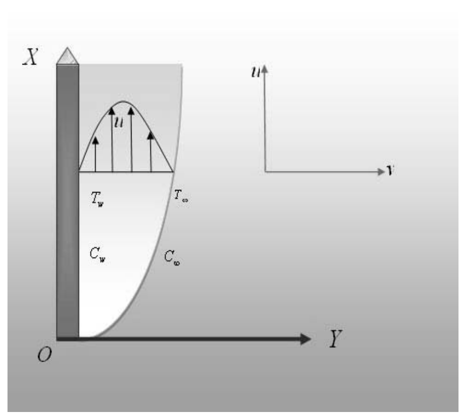

Fig. 1. The physical model and coordinate system

Within the framework of the above stated assumptions with reference to the generalized equations described before the equation relevant to the transient two dimensional problems are governed by the following system of coupled non-linear differential equations.

Continuity equation
$$\frac{\partial u}{\partial x}+\frac{\partial v}{\partial y}=0 \tag{1}$$

Momentum equation
$$\frac{\partial u}{\partial t}+u\frac{\partial u}{\partial x}+v\frac{\partial v}{\partial y}=v\frac{\partial^2 u}{\partial y^2}+g\beta\left(T-T_\infty\right)+g\beta^*\left(C-C_\infty\right) \tag{2}$$

Energy equation
$$\frac{\partial T}{\partial t}+u\frac{\partial T}{\partial x}+v\frac{\partial T}{\partial y}=\frac{K}{\rho C_p}\frac{\partial^2 T}{\partial y^2}+Q\left(T_\infty-T\right) \tag{3}$$

Concentration equation
$$\frac{\partial C}{\partial t}+u\frac{\partial C}{\partial x}+v\frac{\partial C}{\partial y}=D\frac{\partial^2 C}{\partial y^2} \tag{4}$$

With the corresponding initial and boundary conditions are

At $t=0$ $\quad u=0, v=0,\ T\to T_\infty C\to C_\infty$ everywhere (5)

$$\begin{aligned}
&u=0,\ v=0,\ T\to T_\infty,\ C\to C_\infty \quad at\ x=0\\
t>0\quad &u=0,\ v=0,\ T\to T_w,\ C\to C_w \quad at\ y=0\\
&u=0,\ v=0,\ T\to T_w,\ C\to C_w \quad as\ y\to\infty
\end{aligned} \tag{6}$$

where x, y are Cartesian coordinate system. u, v are x, y component of flow velocity respectively is the local acceleration due to gravity ; υ is the kinematic viscosity; ρ is the density of the fluid ; K is the thermal conductivity ; C_p is the specific heat at the constant pressure; D is the coefficient of mass diffusivity.

3. Mathematical Formulation

Since the solutions of the governing equations (1)-(4) under the initial (5) and boundary (6) conditions will be based on a finite difference method it is required to make the said equations dimensionless.

For this purpose we now introduce the following dimensionless variables;

$$X=\frac{xU_0}{\upsilon},\ Y=\frac{yU_0}{\upsilon},\ U=\frac{u}{U_0},\ V=\frac{v}{U_0},\ \tau=\frac{tU_0^2}{\upsilon},\bar{T}=\frac{T-T_\infty}{T_w-T_\infty}\ \text{and}\ \bar{C}=\frac{C-C_\infty}{C_w-C_\infty}$$

Now we substitute the values of the derivatives into the equations (1)-(4) and by simplifying we obtain the following nonlinear coupled partial differential equations in terms of dimensionless variables

$$\frac{\partial U}{\partial X}+\frac{\partial V}{\partial Y}=0 \tag{7}$$

$$\frac{\partial U}{\partial \tau}+U\frac{\partial U}{\partial X}+V\frac{\partial U}{\partial Y}=\frac{\partial^2 U}{\partial Y^2}+G_r\bar{T}+G_m\bar{C} \tag{8}$$

$$\frac{\partial \bar{T}}{\partial \tau}+U\frac{\partial \bar{T}}{\partial X}+V\frac{\partial \bar{T}}{\partial Y}=\frac{1}{\Pr}\frac{\partial^2 \bar{T}}{\partial Y^2}-\alpha\bar{T} \tag{9}$$

$$\frac{\partial \bar{C}}{\partial \tau} + U\frac{\partial \bar{C}}{\partial X} + V\frac{\partial \bar{C}}{\partial Y} = \frac{1}{S_c}\frac{\partial^2 \bar{C}}{\partial Y^2} \tag{10}$$

where, Grashof number $= G_r = \upsilon g \beta \dfrac{(T_w - T_\infty)}{U_0^{\,3}}$

Modified Grashof number $= G_m = \upsilon g^* \beta \dfrac{(C_w - C_\infty)}{U_0^{\,3}}$

Prandlt number $= P_r = \dfrac{\upsilon \rho C_p}{K}$

Schmidt number $= S_c = \dfrac{\upsilon}{D}$

Heat source parameter $\alpha = \dfrac{Q\upsilon}{U_0^2}$

Also the associated initial and boundary conditions become

$$\tau = 0 \qquad U = 0,\ V = 0,\ \bar{T} = 0,\ \bar{C} = 0 \qquad \text{Everywhere} \tag{11}$$

$$\begin{aligned} & U = 0,\ V = 0,\ \bar{T} = 0,\ \bar{C} = 0 \quad at\ X = 0 \\ \tau > 0 \quad & U = 0,\ V = 0,\ \bar{T} = 1,\ \bar{C} = 1 \quad at\ Y = 0 \\ & U = 0,\ V = 0,\ \bar{T} = 0,\ \bar{C} = 0 \quad as\ Y \to \infty \end{aligned} \tag{12}$$

4. Numerical Calculations

In this section, we attempt to solve the governing second order nonlinear coupled dimensionless partial differential equations with the associated initial and boundary conditions. For solving a transient free convection flow with heat and mass transfer past a semi infinite plate, *Callahan* and *Marner* (1976) used the difference method.

From the concept of the above discussion, for simplicity the explicit finite difference method has been used to solve equations (7) - (10) subject to the conditions given by (11) and (12). To obtain the difference equations the region of the flow is divided into a grid of lines parallel to X and Y axes where X -axes is taken along the plate and Y - axes is normal to the plate. Here we consider that the plate of height $X_{max}(=200)$ i.e. X varies from 0 to 200 and regard $Y_{max}(=20)$ as corresponding to $Y \to \infty$ i.e. Y varies 0 to 20. Again, we consider that the plate of height $X_{max}(=100)$ i.e. X varies from 0 to 100 and regard $Y_{max}(=20)$ for $P_r = 0.71$ as corresponding to $Y \to \infty$ i.e. Y varies 0 to 20. Consider $m = 400, n = 400$ in the X and Y axis grid spaces for $P_r = 1.00$ and $P_r = 7.00$. For $P_r = 0.71$ has been taken $m = 200$ and $n = 200$ in the X and Y axis grid spaces as shown in the Fig. 2.

Now $U', V', \overline{T}', \overline{C}'$ are denoted the values of $U, V, \overline{T}, \overline{C}$ at the end of a step of time respectively.

Using the explicit finite difference approximation we get,

$$\left(\frac{\partial U}{\partial \tau}\right)_{i,j} = \frac{U'_{i,j} - U_{i,j}}{\Delta \tau}, \quad \left(\frac{\partial U}{\partial X}\right)_{i,j} = \frac{U_{i,j} - U_{i-1,j}}{\Delta X}, \tag{13}$$

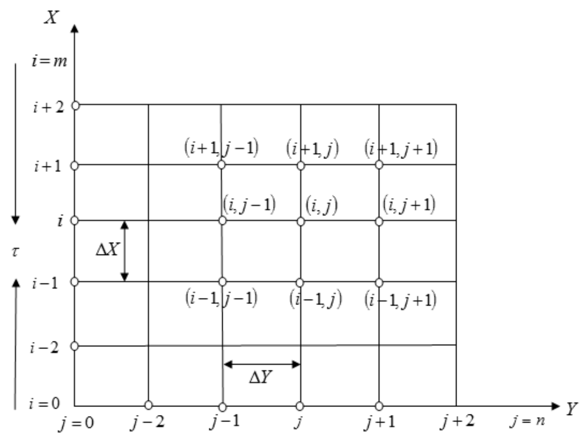

Fig. 2. The finite difference space grid

$$\left(\frac{\partial U}{\partial Y}\right)_{i,j} = \frac{U_{i,j+1} - U_{i,j}}{\Delta Y}, \left(\frac{\partial V}{\partial Y}\right)_{i,j} = \frac{V_{i,j} - V_{i,j-1}}{\Delta Y},$$

$$\left(\frac{\partial \overline{T}}{\partial \tau}\right)_{i,j} = \frac{\overline{T}'_{i,j} - \overline{T}_{i,j}}{\Delta \tau}; \left(\frac{\partial \overline{T}}{\partial X}\right)_{i,j} = \frac{\overline{T}_{i,j} - \overline{T}_{i-1,j}}{\Delta X}; \left(\frac{\partial \overline{T}}{\partial Y}\right)_{i,j} = \frac{\overline{T}_{i,j+1} - \overline{T}_{i,j}}{\Delta Y}$$

$$\left(\frac{\partial \overline{C}}{\partial \tau}\right)_{i,j} = \frac{\overline{C}'_{i,j} - \overline{C}_{i,j}}{\Delta \tau}; \left(\frac{\partial \overline{C}}{\partial X}\right)_{i,j} = \frac{\overline{C}_{i,j} - \overline{C}_{i-1,j}}{\Delta X}; \left(\frac{\partial \overline{C}}{\partial Y}\right)_{i,j} = \frac{\overline{C}_{i,j+1} - \overline{C}_{i,j}}{\Delta Y}$$

$$\left(\frac{\partial^2 U}{\partial Y^2}\right)_{i,j} = \frac{U_{i,j+1} - 2U_{i,j} + U_{i,j-1}}{(\Delta Y)^2}; \left(\frac{\partial^2 \overline{T}}{\partial Y^2}\right)_{i,j} = \frac{\overline{T}_{i,j+1} - 2\overline{T}_{i,j} + \overline{T}_{i,j-1}}{(\Delta Y)^2}$$

$$\left(\frac{\partial^2 \overline{C}}{\partial Y^2}\right)_{i,j} = \frac{\overline{C}_{i,j+1} - 2\overline{C}_{i,j} + \overline{C}_{i,j-1}}{(\Delta Y)^2} \tag{14}$$

Substituting the above relations into the corresponding differential equation we obtain an appropriate set of finite difference equations,

$$\frac{U_{i,j} - U_{i-1,j}}{\Delta X} + \frac{V_{i,j} - V_{i,j-1}}{\Delta Y} = 0$$

$$\therefore V_{i,j} = V_{i,j-1} + \frac{U_{i-1,j} - U_{i,j}}{\Delta X} \Delta Y \tag{15}$$

$$\frac{U'_{i,j}-U_{i,j}}{\Delta\tau}+U_{i,j}\frac{U_{i,j}-U_{i-1,j}}{\Delta X}+V_{i,j}\frac{U_{i,j+1}-U_{i,j}}{\Delta Y}=\frac{U_{i,j+1}-2U_{i,j}+U_{i,j-1}}{\left(\Delta Y\right)^2}+Gr\overline{T}_{i,j}+Gm\overline{C}_{i,j}$$

$$U'_{i,j}=\left[\frac{U_{i,j+1}-2U_{i,j}+U_{i,j-1}}{\left(\Delta Y\right)^2}+Gr\overline{T}_{i,j}+Gm\overline{C}_{i,j}-U_{i,j}\frac{U_{i,j}-U_{i-1,j}}{\Delta X}-V_{i,j}\frac{U_{i,j+1}-U_{i,j}}{\Delta Y}\right]\Delta\tau+U_{i,j} \quad (16)$$

$$\frac{\overline{T}'_{i,j}-\overline{T}_{i,j}}{\Delta\tau}+U_{i,j}\frac{\overline{T}_{i,j}-\overline{T}_{i-1,j}}{\Delta X}+V_{i,j}\frac{\overline{T}_{i,j+1}-\overline{T}_{i,j}}{\Delta Y}=\frac{1}{\Pr}\frac{\overline{T}_{i,j+1}-2\overline{T}_{i,j}+\overline{T}_{i,j-1}}{\left(\Delta Y\right)^2}-\alpha\overline{T}_{i,j} \quad (17)$$

$$\frac{\overline{C}'_{i,j}-\overline{C}_{i,j}}{\Delta\tau}+U_{i,j}\frac{\overline{C}_{i,j}-\overline{C}_{i-1,j}}{\Delta X}+V_{i,j}\frac{\overline{C}_{i,j+1}-\overline{C}_{i,j}}{\Delta Y}=\frac{1}{S_c}\frac{\overline{C}_{i,j+1}-2\overline{C}_{i,j}+\overline{C}_{i,j-1}}{\left(\Delta Y\right)^2}$$

$$\overline{C}'_{i,j}=\left[\frac{1}{Sc}\frac{\overline{C}_{i,j+1}-2\overline{C}_{i,j}+\overline{C}_{i,j-1}}{\left(\Delta Y\right)^2}-U_{i,j}\frac{\overline{C}_{i,j}-\overline{C}_{i-1,j}}{\Delta X}-V_{i,j}\frac{\overline{C}_{i,j+1}-\overline{C}_{i,j}}{\Delta Y}\right]\Delta\tau+\overline{C}_{i,j} \quad (18)$$

The initial and boundary conditions with the finite difference scheme are

$$U^0_{i,j}=0,\ V^0_{i,j}=0,\ \overline{T}^0_{i,j}=0,\ \overline{C}^0_{i,j}=0 \quad (19)$$

$$\begin{aligned} U^n_{0.j}&=0,\ V^n_{0,j}=0,\ \overline{T}^n_{0,j}=0,\ \overline{C}^n_{0,j}=0\\ U^n_{i,0}&=0,\ V^n_{i,0}=0,\ \overline{T}^n_{i,0}=1,\ \overline{C}^n_{i,0}=1 \quad (20)\\ U^n_{i,L}&=0,\ V^n_{i,L}=0,\ \overline{T}^n_{i,L}=0,\ \overline{C}^n_{i,L}=0\end{aligned}$$

where $L\to\infty$

Here the subscripts i and j designate the grid points with x and y coordinates respectively and the superscript n represents a value of time, $\tau=n\Delta\tau$ where $n=0,1,2,3........$ From the initial condition (11), the values of $U,\overline{T},\overline{C}$ is known at $\tau=0$. During any one time step, the coefficients $U_{i,j}$ and $V_{i,j}$ appearing in equations (13)-(14) are created as constants. Then at the end of any time-step $\Delta\tau$ the temperature $\overline{T'}$, the concentration $\overline{C}'$,the new velocity U', the new induced field V' at all interior nodal points may be obtained by successive applications of equations (15) - (18) respectively. This process is repeated in time and provided the time-step is sufficiently small, U, V, $\overline{T}$, $\overline{C}$ should eventually converge to values which approximate the steady-state solution of equations (15)-(18). These converged solutions are shown graphically in figures.

5. Results and Discussion

The main goal of the computation is to obtain the steady state solutions for the non-dimensional velocity U, temperature $\overline{T}$ and concentration $\overline{C}$ for different values of Prandtl number $\left(\Pr\right)$, Grashof number $\left(Gr\right)$ Modified Grashof number $\left(Gm\right)$ Schmidt number(Sc) Heat source parameter(α). For this purpose computations have been carried out up to dimensionless time τ = 80. The results of the computations, however, show graphical changes in the below mentioned quantities to time τ =40 have been reached and after this at $\tau = (50-80)$ graphical change negligible. Thus the solution for dimensionless time τ =80 is essentially steady state solutions. Along with the steady state solutions the solutions for the transient values of U versus Y ,$\overline{T}$ versus Y, $\overline{C}$ versus Y are shown in below for different values of parameters. Three values of prandtl number are considered as 0.71, 1.0 and 7.0. Here, Pr = 0.71 represent air at 20^0, Pr =1.0 correspond to electrolyte solutions(such as salt water) and Pr =7.0 represents water. Three values of Schmidt number (*Sc*), Grashof number (*Gr*), Modified Grashof number (*Gm*) and heat source parameter (α) are however chosen arbitrarily.

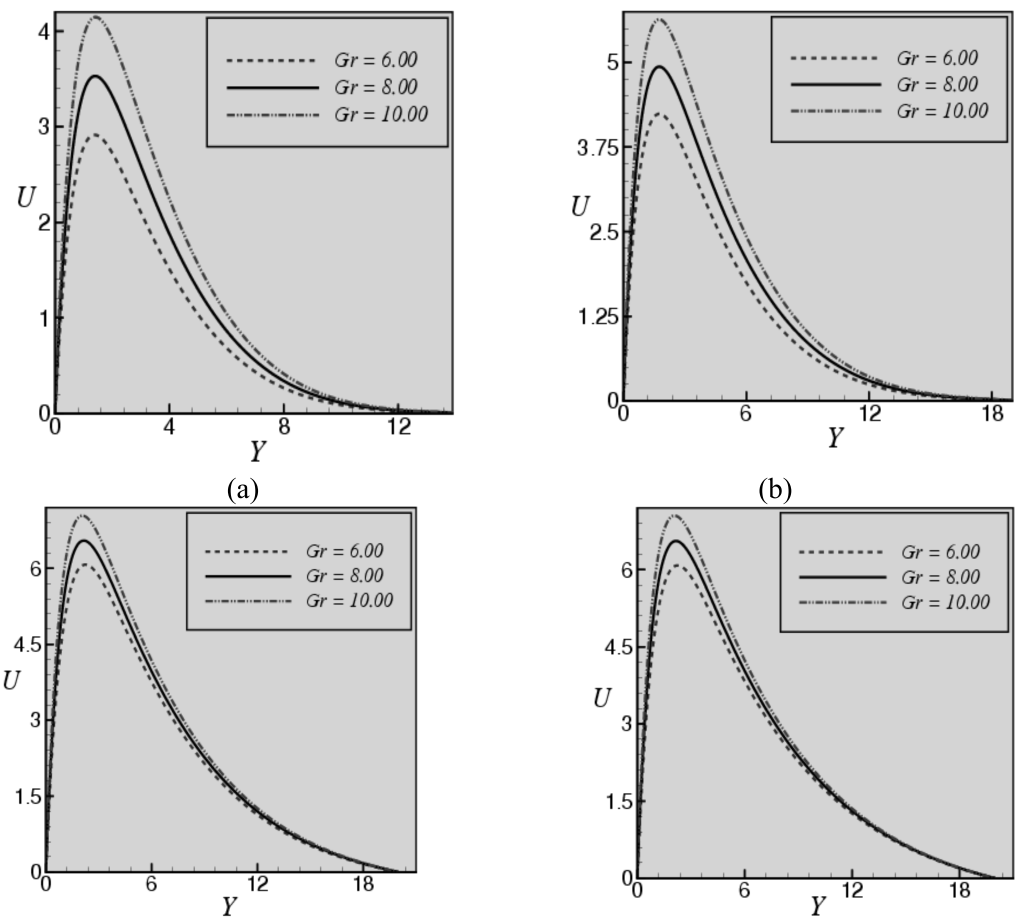

(c) (d)

Fig. 3. Velocity profile for different values of Grashof number at $\Pr = 1.00$, $\alpha = 2.00$, $Gm = 3.00$, $Sc = 15.00$ (a) at time $\tau = 10$ (b) at time $\tau = 20$ (c) at time $\tau = 50$ (d) at time $\tau = 80$

From Fig. 3(a) we observe that the velocity profile increases with the increase of *Gr* at time $\tau = 10$ and with the increasing of time the velocity profile remain unchanged which is shown by Fig. 3(b), Fig.3(c) and Fig. 3(d).

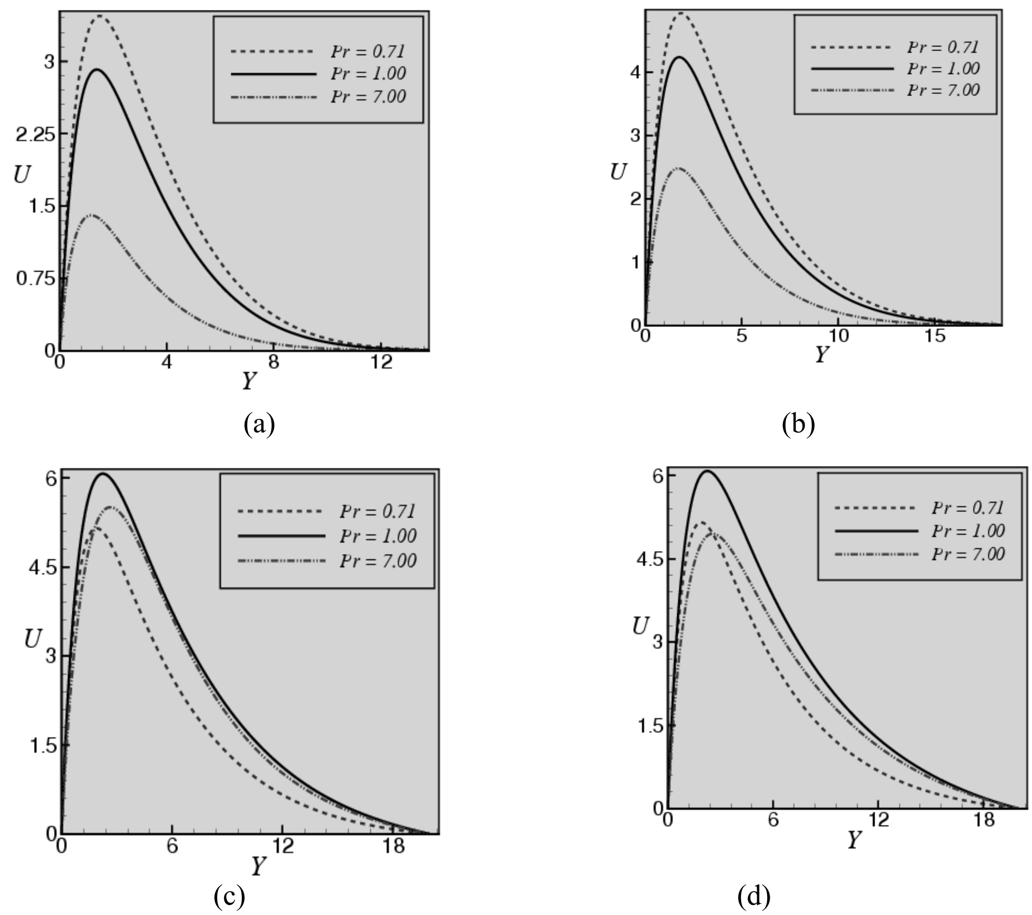

Fig. 4. Velocity profile for different values of Prandtl number at $\alpha = 2.00$, $Gr = 6.00$, $Gm = 3.00$, $Sc = 15.00$ (a) at time $\tau = 10$ (b) at time $\tau = 20$ (c) at time $\tau = 50$ (d) at time $\tau = 80$.

Fig. 4(a) and Fig. 4(b) shows that the velocity profile decreases with the increases of *Pr* at time $\tau = 10, 20$ but at time $\tau = 50, 80$ the velocity profile increases at *Pr* = 0.71, 1.00 which is shown by Fig. 4(c) and Fig. 4(d). We also observed that velocity profile decreases at *Pr* = 7.00 at time $\tau = 50, 80$

Fig. 5 shows that the effects of temperature at various *Pr* with respect to time. We observed that the temperature profile decreases with the increases of *Pr* at different time. We observed that the rate of change temperature at *Pr* = 7.0 is low.

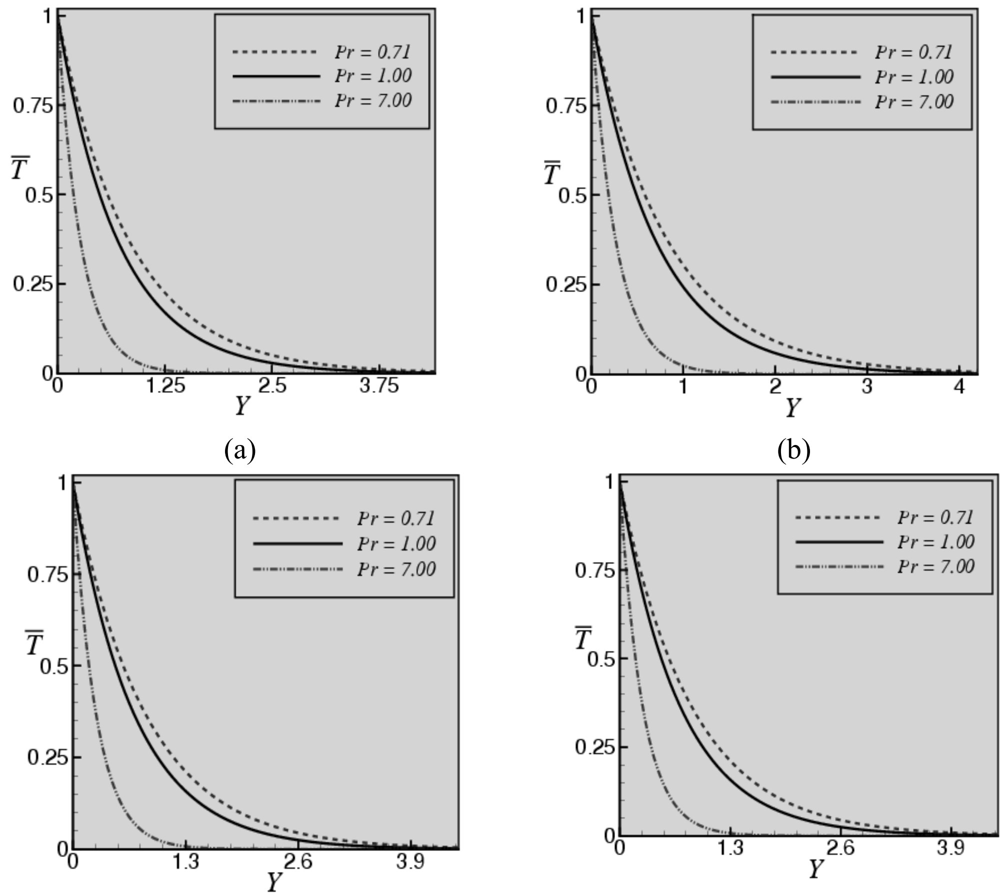

(a) (b)

(c) (d)

Fig. 5. Temperature profile for different values of Prandtl number at $\alpha = 2.00$, $Gr = 6.00$, $Gm = 3.00$, $Sc = 15.00$ (a) at time $\tau = 10$ (b) at time $\tau = 20$ (c) at time $\tau = 50$ (d) at time $\tau = 80$.

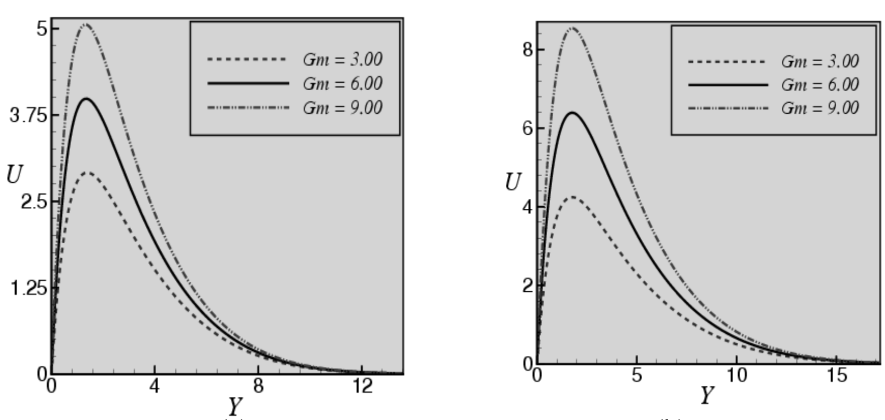

(a) (b)

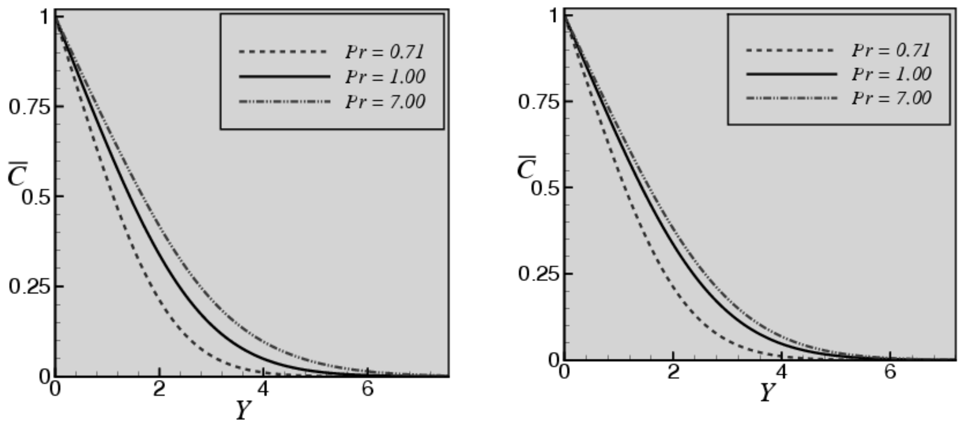

(c) (d)

Fig. 6. Concentration profile for different values of Prandtl number at $\alpha = 2.00$, $Gr = 6.00$, $Gm = 3.00$, $Sc = 15.00$ (a) at time $\tau = 10$ (b) at time $\tau = 20$ (c) at time $\tau = 50$ (d) at time $\tau = 80$.

Fig. 6 shows that the concentration profile for different values of *Pr* and from Fig. 6(a) and Fig. 6(b) we found that the concentration profile is steady at time $\tau = 10, 20$ but Fig. 6(c) and Fig. 6(d) shows that the concentration profile increases with the increases of *Pr* at time $\tau = 50, 80$.

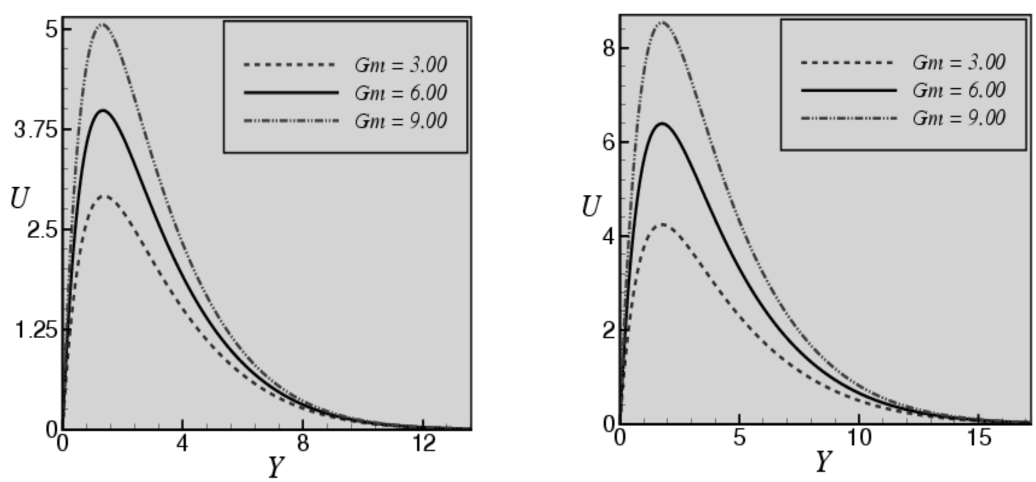

(a) (b)

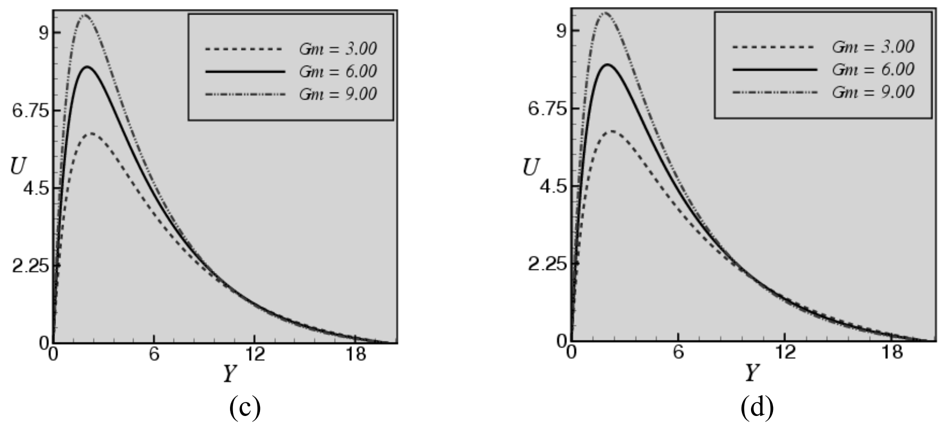

Fig. 7. Velocity profile for different values of Modified Grashof number at $\Pr = 1.00$, $\alpha = 2.00$, $Gr = 6.00$, $Sc = 15.00$ (a) at time $\tau = 10$ (b) at time $\tau = 20$ (c) at time $\tau = 50$ (d) at time $\tau = 80$

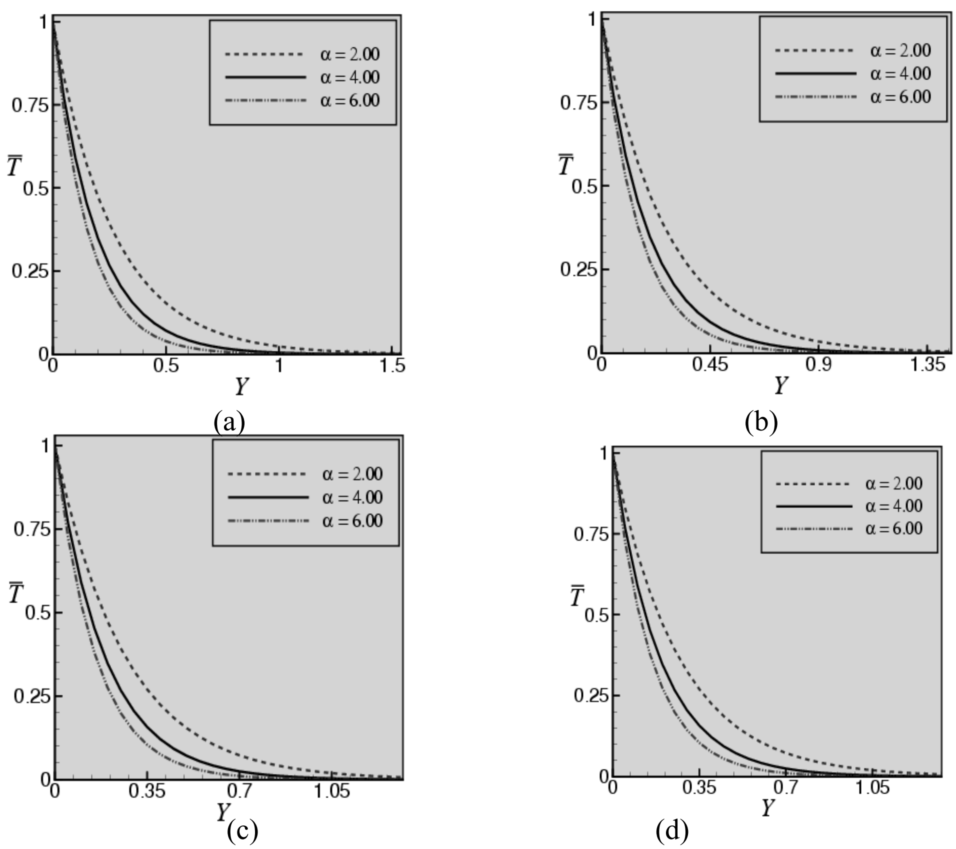

Fig. 8. Temperature profile for different values of Heat source parameter(α) at $\Pr = 7.00$, $Gm = 3.00$, $Gr = 6.00$, $Sc = 15.00$ (a) at time $\tau = 10$ (b) at time $\tau = 20$ (c) at time $\tau = 50$ (d) at time $\tau = 80$.

Fig. 7 represents the velocity profile for different values of Modified Grashof number at different time. We observed that velocity profile increases with the increases of *Gm* at different time.

Fig. 8 represents the temperature profile for different values of heat source parameter (α) at different time. We observed that temperature profile decreases with the increases of α at different time.

6. Conclusion

In this paper, we studied equation of continuity and derived the Navier-Stokes (N-S) equations of motion for viscous compressible and incompressible fluid flow for different co-ordinate system. Then we performed the boundary layer equation in two-dimensional flow, energy equation, mass transfer/concentration equation and thermal boundary layer equation.

Finally, the thermal boundary layer equations have been derived from Navier-Stokes and concentration equation by boundary layer technique. Boundary layer equations have been non-dimensionalised by using non-dimensional variable. The non-dimensional boundary layer equations are non-linear partial differential equations. These equations are solved by using finite difference method. Finite difference solution of heat and mass transfer flow is studied to examine the velocity, temperature and concentration distribution characteristics. The effect on the velocity, temperature and concentration for the various parameters entering into the problems are separately discussed with the help of graphs. Then the results in the form of velocity, temperature and concentration distribution are shown graphically.

To obtain the steady-state solutions for the non-dimensional velocity U, temperature $\overline{T}$ and concentration $\overline{C}$ we use different values of Prandtl number $(\Pr)$, Grashof number (Gr), Modified Grashof number (Gm), Schmidt number (Sc) and Heat source parameter (α). For this purpose, computations have been carried out up to dimensionless time τ =10, 20, 50, 80. Along with the steady state solutions, the solutions for the transient values of U versus Y, $\overline{T}$ versus Y and $\overline{C}$ versus Y are obtained. The results of the computations, however, show graphical changes in the mentioned quantities to time τ = 40 have been reached and after this at $\tau = (50-80)$ graphical change are negligible. Thus the solution for dimensionless time τ = 80 are essentially steady-state solutions.

REFERENCES

1. S. V. Patankar and D. B. Spalding, *International Journal of Heat and Mass Transfer,* 10 (1967), 1389-1411.
2. M. S. Alam, M. M. Rahman and M. A. Samad, Numerical Study of the Combined Free-Forced Convection and Mass Transfer Flow Past a Vertical Porous Plate in a Porous Medium with Heat Generation and Thermal Diffusion, *Nonlinear Analysis: Modeling and Control,* 11(4) (2006), 331-343.

3. M. M. Alam, M. R. Islam and F. Rahman, Study Heat and Mass Transfer by Mixed Convection Flow from a Vertical Porous Plate with Induced Magnetic Field, Constant Heat and Mass Fluxes, *Thammasat Int. J. of Science and Technology*, 13(4) (2008),1-13.
4. Md. Mahamud Alam and M. A. Sattar, *Journal of Energy, Heat and Mass Transfer,* 21 (1999), 9-21.
5. M. M. Alam, M. M. Haque, M. Delowar Hossainb and Z. Haque, Combined Heat and Mass Transfer by Mixed Convection Unsteady MHD Flow with Constant Heat and Mass Fluxes, *Bangladesh J. Sci. Ind. Res.,* 43(3), (2008), 309-320.
6. Pratap Rudra, *A Quick Introduction for Scientists and Engineers*, Oxford University Press, (2006).
7. L. Prandtl, *The mechanics of viscous fluids*, Division G., Vol. III Aerodynamic theory, edited by W.F. Durand, Julius Springer, Berlin, (1935).
8. K. R. Rajput and S. Chand, *Heat and Mass Transfer,* S. Chand & Company Ltd. (2007).
9. M. A. Sattar and M.M. Alam, *Indian Journal of Pure and Applied Mathematics,* 25(6) (1994), 679.